

RESEARCH ARTICLE

Fish embryo vulnerability to combined acidification and warming coincides with a low capacity for homeostatic regulation

Flemming Dahlke^{1,2,*}, Magnus Lucassen¹, Ulf Bickmeyer¹, Sylke Wohlrab^{1,3}, Velmurugu Puvanendran⁴, Atle Mortensen⁴, Melissa Chierici⁵, Hans-Otto Pörtner^{1,2} and Daniela Storch¹

ABSTRACT

The vulnerability of fish embryos and larvae to environmental factors is often attributed to a lack of adult-like organ systems (gills) and thus insufficient homeostatic capacity. However, experimental data supporting this hypothesis are scarce. Here, by using Atlantic cod (*Gadus morhua*) as a model, the relationship between embryo vulnerability (to projected ocean acidification and warming) and homeostatic capacity was explored through parallel analyses of stage-specific mortality and *in vitro* activity and expression of major ion pumps (ATP-synthase, Na⁺/K⁺-ATPase, H⁺-ATPase) and co-transporters (NBC1, NKCC1). Immunolocalization of these transporters was used to study ionocyte morphology in newly hatched larvae. Treatment-related embryo mortality until hatching (+20% due to acidification and warming) occurred primarily during an early period (gastrulation) characterized by extremely low ion transport capacity. Thereafter, embryo mortality decreased in parallel with an exponential increase in activity and expression of all investigated ion transporters. Significant changes in transporter activity and expression in response to acidification (+15% activity) and warming (−30% expression) indicate some potential for short-term acclimatization, although this is probably associated with energetic trade-offs. Interestingly, whole-larvae enzyme activity (supported by abundant epidermal ionocytes) reached levels similar to those previously measured in gill tissue of adult cod, suggesting that early-life stages without functional gills are better equipped in terms of ion homeostasis than previously thought. This study implies that the gastrulation period represents a critical transition from inherited (maternal) defenses to active homeostatic regulation, which facilitates enhanced resilience of later stages to environmental factors.

KEY WORDS: Ocean acidification, Early-life history, Ion regulation, Energy allocation, Critical period, Gastrulation, Atlantic cod

INTRODUCTION

Embryonic development is a critical period in the lifecycle of most organisms (Hamdoun and Epel, 2007). This could be particularly

true for ectothermic species that release their eggs into the ocean (Przeslawski et al., 2015), which is expected to warm and acidify at an unprecedented rate over the coming decades (IPCC, 2019). The vulnerability of embryos and early larvae to climatic changes (and environmental factors in general) is often attributed to a lack of adult-like organ systems involved in energy and ion homeostasis (Melzner et al., 2009b; Hamdoun and Epel, 2007). However, knowledge about the development of homeostatic capacity and its contribution to environmental tolerance is still incomplete (Burggren and Bautista, 2019), making it difficult to identify lifecycle bottlenecks and climatic risks (Burggren and Mueller, 2015; Esbaugh, 2018).

The eggs of aquatic ectotherms such as fish are permeable to dissolved gases (e.g. O₂ and CO₂) and thermally equilibrated with their environment (Finn and Kapoor, 2008). Embryos are therefore directly exposed to changes in water temperature and CO₂-driven acidification without having regulatory (defensive) organ systems like gills (Finn and Kapoor, 2008). Instead, early (cleavage) stages are thought to be protected by maternally provisioned (passive) defenses such as non-bicarbonate pH buffering and constitutive heat-shock proteins (Melzner et al., 2009b; Hamdoun and Epel, 2007). These mechanisms may support embryonic resilience to natural environmental variability (Hamdoun and Epel, 2007), but the level of innate robustness is probably species specific and, in some cases, insufficient to cope with the challenges posed by anthropogenic climate change (Przeslawski et al., 2015; Dahlke et al., 2017). After the cleavage stage, developmental control and defense are transferred from maternal factors to those synthesized from the embryonic genome (Tadros and Lipshitz, 2009), and it is expected that the progressive differentiation of specialized cells (ionocytes) and tissues promotes active homeostatic regulation and thus improved environmental tolerance (Alderdice, 1988; Rombough, 1997; Melzner et al., 2009b).

As inferred from studies on adult fish, maintenance of homeostasis in a thermally dynamic environment includes adjustments to the structure and functioning of cell membranes and enzymes involved in energy (ATP) production (Somero et al., 2017). Within temperature limits that are typically narrow in embryos and larvae (Rombough, 1997), such responses (i.e. thermal acclimatization) may support normal development and optimal use of energetic resources (Schnurr et al., 2014; Scott et al., 2012). Developmental defects can result from a mismatch between ATP demand and supply capacity at critically high or low temperatures (Sokolova et al., 2012; Dahlke et al., 2017; Leo et al., 2018), as well as from thermal damage to proteins at extreme temperatures (Somero, 2010). CO₂-driven acidification hampers the diffusive release of metabolic CO₂ across epithelial surfaces, which causes an increase in internal P_{CO₂} and, consequently, a potentially harmful decline in pH of extracellular/intracellular body fluids (Brauner et al., 2019). Restoring acid–base balance requires ATP-intensive

¹Alfred Wegener Institute, Helmholtz Centre for Polar and Marine Research, Am Handelshafen 12, 27570 Bremerhaven, Germany. ²University of Bremen, NW 2 Leobener Str., 28359 Bremen, Germany. ³Helmholtz Institute for Functional Marine Biodiversity, Ammerländer Heersstraße 231, 26129 Oldenburg, Germany. ⁴Nofima AS, Muninbakken 9, 9019 Tromsø, Norway. ⁵Institute of Marine Research, Fram Centre, 9019 Tromsø, Norway.

*Author for correspondence (flemming.dahlke@awi.de)

 F.D., 0000-0003-0095-2362; M.L., 0000-0003-4276-4781; U.B., 0000-0002-5351-2902; S.W., 0000-0003-3190-0880; V.P., 0000-0002-4416-7000; A.M., 0000-0001-8735-7819; M.C., 0000-0003-0222-2101; H.-O.P., 0000-0001-6535-6575; D.S., 0000-0003-3090-7554

ion transport mechanisms (Pörtner, 2008), including proton (H^+) excretion and bicarbonate (HCO_3^-) accumulation (Brauner et al., 2019). The additional ATP demand for CO_2 compensation is expected to reduce embryonic/larval growth efficiency and thermal tolerance by tightening energy supply constraints at critical temperatures (Pörtner, 2008; Dahlke et al., 2017; Dahlke et al., 2018). Increased climate vulnerability of embryos and larvae compared with adults probably represents a common feature among vertebrate and invertebrate taxa living in different climate zones and habitats (Rombough, 1997; Przeslawski et al., 2015). Knowledge regarding the ontogeny of regulatory functions in relation to environmental tolerance, acclimation potential and energy budgeting may help advancing the concept of early-life vulnerability and its potential for directing future eco-physiological research.

Here, we used a marine cold-water fish (Atlantic cod, *Gadus morhua*) to investigate (i) whether vulnerability to end-of-century acidification (increase in P_{CO_2} from 400 to 1100 μatm , -0.4 pH) and warming ($+3.5^\circ\text{C}$; Fig. 1A,B) during early embryogenesis coincides with low homeostatic capacity, and (ii) whether this environmental challenge modifies the development of energy-intensive homeostatic functions, which can inform about acclimatization potential (Burggren, 2018). Embryo vulnerability was quantified

based on daily mortality rates until hatching. Homeostatic capacity was assessed at five stages until yolk sac absorption (Fig. 1C) through measurements of ion transport and ATP synthesis capacity [*in vitro* enzyme activity and/or protein expression of mitochondrial F_1F_0 -ATP-synthase (hereafter ATP-synthase), Na^+/K^+ -ATPase (NKA), V-Type H^+ -ATPase (VHA), Na^+/HCO_3^- cotransporter 1 (NBC1) and $Na^+/K^+/2Cl^-$ cotransporter 1 (NKCC1)] in combination with immunohistological analyses of ionocyte morphology. Cod represents a suitable model because rearing methodology (Puvanendran et al., 2015; Dahlke et al., 2017) and protocols for biochemical analyses and immunolocalization of relevant ion transporters are well established (e.g. Kreiss et al., 2015; Michael et al., 2016b). Furthermore, our previous experiments confirmed the vulnerability of cod embryos to acidification and warming (Dahlke et al., 2017), and data available on ion-regulatory mechanisms in gill tissue of adult cod (e.g. Kreiss et al., 2015; Michael et al., 2016b) allow for quantitative and qualitative comparisons between embryos, larvae and adults.

MATERIALS AND METHODS

This experiment was conducted in Norway in 2014 according to local regulations of the Norwegian Animal Research Authority (Forsøksdyrutvalget, permit: FOTS ID 6382).

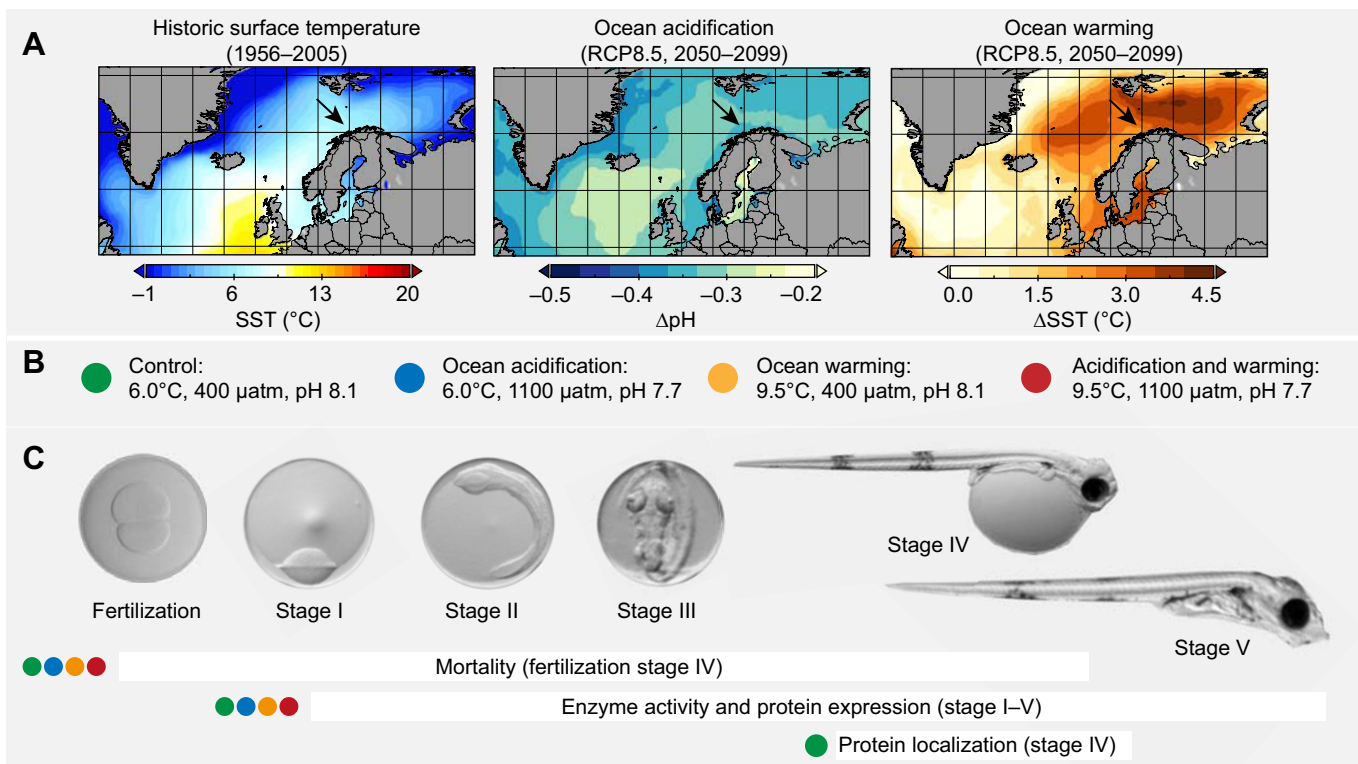


Fig. 1. Experimental design. (A) Adult Atlantic cod, *Gadus morhua*, used in this experiment were caught in the Barents Sea off the coast of northern Norway (black arrows). The maps show historic sea surface temperature (SST) during the spawning season (March–April) as well as projected ocean acidification (OA) and warming by the end of this century under the IPCC high-emission scenario RCP8.5 (Van Vuuren et al., 2011). Climate data were retrieved from NOAA's climate change web portal (Scott et al., 2016). (B) Six egg batches (produced by $n=6$ different females) were separately incubated from fertilization to yolk sac absorption under four treatment conditions (see also Fig. S1), representing present spawning conditions (6.0°C , $400 \mu\text{atm}$, pH 8.1, green) as well as future OA (6.0°C , $1100 \mu\text{atm}$, pH 7.7, blue), warming (9.5°C , $400 \mu\text{atm}$, pH 8.1, yellow) and the combination of the two factors (9.5°C , $1100 \mu\text{atm}$, pH 7.7, red). (C) Images show developmental stages investigated during this study. The incubation experiment was terminated at the stage of yolk sac absorption (stage V, 24 days at 6.0°C , 15 days at 9.5°C). Daily embryo mortality was assessed between 12 h post-fertilization and the onset of hatching (stage IV). Enzyme activity and protein expression of major ion transporters were determined at stages I–V. Ion transporters were immunolocalized in larvae (stage IV) reared under control conditions.

Experimental animals

Mature Atlantic cod, *Gadus morhua* Linnaeus 1758, were caught by longlining in the southern Barents Sea (Tromsøflaket, approximately 70.5°N, 18°E) in March 2014. After being transported to the Centre for Marine Aquaculture of Nofima outside Tromsø (Norway), the fish were held in a flow-through tank (25 m³, supplied with fjord water) under ambient photoperiod, salinity (34 ppt), pH (8.1) and temperature (5–6°C) conditions.

Fertilization

Gametes used for *in vitro* fertilization were obtained by means of strip spawning from randomly selected females ($n=6$, 66–94 cm length) and males ($n=12$, 59–91 cm length; Table S1). All fertilizations were conducted within 30 min of stripping according to a standard protocol (Brown et al., 2003). In brief, each of six egg batches was divided into two equal portions to be fertilized under two different P_{CO_2} conditions (400 and 1100 μatm , $\text{pH}_{\text{FreeScale}}$ 8.1 and 7.7) using filtered (0.2 μm) seawater adjusted to 6°C. To maximize genetic diversity, the eggs of each female were fertilized with a sperm mix from two different males. Fertilization success (Table S1) was determined in subsamples of 100 eggs ($n=3$ subsamples per batch and P_{CO_2} treatment), which had been incubated in sealed Petri dishes (20 ml water volume) for 12 h at 6°C before being photographed with a digital camera mounted to a binocular. Eggs (8 or 16 cell stage) with a clear and regular cleavage pattern were considered fertilized.

Incubation

A full-factorial design with two levels of P_{CO_2} /pH (400 μatm , pH 8.1 and 1100 μatm , pH 7.7) and two temperatures (6 and 9.5°C) was used for incubation of eggs and larvae (Fig. S1). Eggs previously fertilized at different P_{CO_2} conditions were subdivided into different temperature groups with the same P_{CO_2} , resulting in four experimental treatments: (i) 6°C, 400 μatm ; (ii) 6°C, 1100 μatm ; (iii) 9.5°C, 400 μatm ; and (iv) 9.5°C, 1100 μatm . Eggs for treatments iii and iv were warmed from 6°C to 9.5°C at a rate of $\sim 0.5^\circ\text{C h}^{-1}$. Increased temperature and P_{CO_2} conditions reflect end-of-century climate projections according to the IPCC high-emission scenario RCP8.5 (Van Vuuren et al., 2011). Treatment combinations were established in a flow-through incubation system, which consisted of 24 upwelling incubators (6 egg batches \times 2 P_{CO_2} \times 2 temperatures = 24) with a volume of 25 l each. The flow rate was set to 1.5 l min^{-1} to ensure even distribution and mixing of eggs within the incubator. Two flow-through header tanks (150 l volume, one for each temperature) were connected to the water supply pipes and equipped with a multi-channel feedback system (IKS-Aquastar, IKS, Karlsbad, Germany) to adjust (and control) elevated pH/ P_{CO_2} values online via infusion of pure CO_2 . Automatic recordings (every 30 min) of temperature and pH values within the incubation systems were referenced against daily

measurements of seawater pH/temperature with a laboratory-grade pH-electrode (InLab Routine Pt 1000, Mettler Toledo, Columbus, OH, USA) connected to a WTW 3310 pH-meter (Weilheim, Germany). Prior to each measurement, the electrode was recalibrated against tempered Tris–HCl seawater buffers (Dickson et al., 2007) to convert pH_{NBS} readings to the free proton concentration scale of seawater pH (pH_{F}) (Waters and Millero, 2013). The CO2SYS program (Lewis et al., 1998) was used to calculate P_{CO_2} values based on total alkalinity and dissolved inorganic carbon determined in water samples ($n=3$) from each treatment combination (taken during the running experiment). Seawater parameters are summarized in Table 1.

Embryo mortality

Egg batches ($n=6$, 200–520 ml; Table S1) were equally distributed across treatments (50–130 ml per incubator). Egg mortality was determined volumetrically every 24 h until the onset of hatching by draining dead (sunken) eggs into a graduated cylinder (± 0.5 ml). Fertilization success data (Table S1) were used to estimate the volume of fertilized and unfertilized eggs within each incubator. Daily mortality rates were calculated as percentages relative to the estimated volume of eggs that was present in the incubator on the previous day. To better resolve changes in embryo vulnerability in relation to developmental age, egg mortality was also displayed as a function of degree-days (days post-fertilization multiplied by incubation temperature) (Trudgill et al., 2005). Total embryo mortality was calculated as the percentage of fertilized eggs that died until hatching stage.

Sampling

Subsamples of eggs and larvae used for analyses of enzyme activity and protein expression were obtained from each treatment at developmental stages I–V (Fig. 1C). These stages were chosen because they represent developmental landmarks that can be reliably identified under a stereomicroscope: stage I: end of cleavage period, stage II: end of gastrulation period, stage III: 50% eye pigmentation, stage IV: peak-hatching, stage V: complete yolk sac absorption (Hall et al., 2004). Developmental progress was monitored in each incubator every 12 h. Prior to sampling, the aeration and water supply of the incubators was turned off so that eggs and larvae accumulated at the water surface. Eggs and larvae were then concentrated within a small kitchen sieve, pipetted into 1.5 ml cryovials (~ 500 individuals per vial) and immediately frozen in liquid nitrogen after excess water was removed by pipetting. Larvae were previously centrifuged to the bottom of the vial (~ 3 s at 500 rpm). Additional samples of larvae (stage IV) reared under control conditions (6°C, 400 μatm) were fixed in 4% buffered formaldehyde (pH 7.4) and stored in 70% phosphate-buffered saline (PBS)-buffered isopropanol (pH 7.4) for immunolocalization of NKA, VHA, ATP-synthase, NBC1 and NKCC1.

Table 1. Seawater temperature and pH of the different treatments

Nominal treatment	Temperature (°C)				pH				P_{CO_2} (μatm)
	Automatic		Manual		Automatic (NBS)		Manual (free scale)		
	Mean	Range	Mean	Range	Mean	Range	Mean	Range	
6.0°C, 400 μatm	6.15	5.8–6.4	6.09	5.95–6.2	8.12	7.93–8.25	8.10	8.08–8.13	380 \pm 7
6.0°C, 1100 μatm					7.74	7.50–7.89	7.72	7.70–7.74	1132 \pm 49
9.5°C, 400 μatm	9.63	9.4–9.8	9.54	9.38–9.70	8.13	7.91–8.25	8.12	8.08–8.16	468 \pm 18
9.5°C, 1100 μatm					7.73	7.55–7.91	7.73	7.63–7.78	1149 \pm 4

Data were recorded automatically every 30 min and checked manually once a day. Mean \pm s.d. P_{CO_2} values were determined in $n=3$ subsamples.

Sample preparation

Crude extract preparation followed the same protocol as described elsewhere (Kreiss et al., 2015; Melzner et al., 2009a; Michael et al., 2016a,b), with the exception that different sample-to-extraction buffer dilutions were applied for egg (stage I–III) and larval (stage IV and V) stages to ensure similar concentrations of biologically active tissue in all extracts. This adjustment was necessary because a given fresh mass of egg-shelled embryos contains approximately half the number of individuals (tissue) than the same mass of frozen larvae (many individuals compressed into one). Given that soluble protein content of egg and early larval stages was reported to vary by less than 3% (Finn et al., 1995), we normalized all measurements against protein content of the crude extract to account for potential differences in the number of individuals per sample. In brief, crude extracts were produced by homogenizing ~100 mg of frozen sample suspended in 5 (eggs) or 10 (larvae) volumes of ice-cold extraction buffer, which contained 50 mmol l⁻¹ imidazole (pH 7.8), 250 mmol l⁻¹ sucrose, 5 mmol l⁻¹ Na₂-EDTA, 0.1% sodium deoxycholate, 5 mmol l⁻¹ β-mercaptoethanol and 0.2 ml proteinase inhibitor cocktail (Sigma-Aldrich, Taufkirchen, Germany; catalog no. P8340). Samples were homogenized in a temperature-controlled tissue homogenizer (Precellys 24, Bertin Technologies, Aix-en-Provence, France) set to 0°C, 6000 rpm (3×15 s). Cell fragments were removed by centrifugation (1000 g for 10 min at 2°C) and the supernatant (crude extract) was taken for analysis. Final protein concentration of the crude extracts were determined according to Bradford (1976), using bovine serum albumin (BSA) as standard. Differences in protein concentration between treatments were not significant (Fig. S2A, Table S3). Half of each sample was used for the enzyme assay and the other half for immunoblotting procedures.

Enzyme assay

Maximum total ATPase activity and fractional (inhibitor-sensitive) activity of NKA, VHA and ATP-synthase (reversed catalysis) were measured in crude extracts by means of a coupled enzyme assay based on pyruvate kinase (PK) and lactate dehydrogenase (LDH) as described elsewhere (Kreiss et al., 2015; Melzner et al., 2009a; Michael et al., 2016a,b). Transporter specific enzyme activity was determined as the difference between total ATPase (TA) activity and inhibitor-insensitive (residual) ATPase activity, using inhibitor concentrations previously applied to gill tissue samples of adult cod: 5 mmol l⁻¹ ouabain for NKA (Michael et al., 2016a), 60 μmol l⁻¹ oligomycin for ATP-synthase (Michael et al., 2016b) and 0.1 μmol l⁻¹ bafilomycin A1 for VHA (Kreiss et al., 2015). The assay was conducted in a micro-plate reader format under temperature-controlled conditions. Samples from 6.0 or 9.5°C incubations were assayed at both temperatures to assess acclimation effects on enzyme activity. The reaction process (oxidation of NADH, hydrolysis of ATP) was initiated by the addition of crude extract to 20 volumes of reaction buffer containing 100 mmol l⁻¹ imidazole, pH 7.8, 80 mmol l⁻¹ NaCl, 20 mmol l⁻¹ KCl, 5 mmol l⁻¹ MgCl₂, 5 mmol l⁻¹ ATP, 0.24 mmol l⁻¹ Na-NADH₂, 2 mmol l⁻¹ phosphoenolpyruvate and 12 U ml⁻¹ PK with 17 U ml⁻¹ LDH in a PK/LDH enzyme mix (Sigma-Aldrich). All samples were arranged in a randomized order and measured in quadruplicate with 10 readings over a time period of 10 min at λ=339 nm. Inhibitor-insensitive activity was calculated based on the extinction coefficient of NADH (ε=6.31 l mmol⁻¹ cm⁻¹) and expressed as micromoles of ATP consumed per mg protein in the crude extract per hour (μmol ATP mg⁻¹ protein h⁻¹).

Antibody specificity

The specificity of all primary antibodies used for protein quantification and/or localization was confirmed by western blotting (Fig. S3). Antibodies against NKA, NKCC1 and NBC1 were previously used to study ion regulation processes in gill tissue of cod (Kreiss et al., 2015; Melzner et al., 2009a; Michael et al., 2016b). The polyclonal antibody against NBC1 was developed specifically for cod (Michael et al., 2016b). Details on primary antibodies are given in Table S2. A mix of subsamples from randomly selected crude extracts (developmental stage IV) was split into membrane and cytosolic fractions by ultra-centrifugation (350,000 g for 30 min at 4°C). A 15 μl sample from each fraction was separated by SDS-PAGE on 8–10% polyacrylamide gels according to Laemmli (1970), and transferred onto PVDF membranes (Immuno-BlotTM, Bio-Rad, Munich, Germany) using a tank blotting system (Bio-Rad). To prevent non-specific protein binding, blots were quenched for 1 h at room temperature (RT) in TBS-Tween buffer [TBS-T, 50 mmol l⁻¹ Tris-HCl, pH 7.4, 0.9% (w/v) NaCl, 0.1% (v/v) Tween20] containing 5% (w/v) non-fat skimmed milk powder. Incubation of blots with primary antibodies was done overnight at 2°C (dilutions in TBS-T are given in Table S2). After washing with TBS-T, blots were incubated for 1 h (RT) with horseradish-conjugated goat anti-rabbit/anti-mouse IgG antibody (Pierce, Rockford, IL, USA, diluted 1:50,000 in TBS-T). Protein bands were visualized with ECL Advanced Western Blotting Detection Reagent (GE Healthcare, Munich, Germany), and imaged with a cooled charge-coupled device camera (LAS-1000: Fuji, Tokyo, Japan). Protein bands (Fig. S3) were referenced to pre-labelled SDS-PAGE standards (Bio-Rad).

Protein quantification

A 48-fold slot-blot filtration system (Hoefer PR 648, Amersham Biosciences, Freiburg, Germany) was used to quantify the expression of NKA, ATP-synthase, NBC1 and NKCC1. VHA was excluded because of insufficient antibody reactivity. After activation in 100% methanol, PVDF membranes were equilibrated for 30 min in transfer buffer [10 mmol l⁻¹ NaHCO₃, 3 mmol l⁻¹ Na₂CO₃, 20% (v/v) methanol, 0.025% (w/v) SDS, pH 9.5–9.9]. Crude extracts were diluted 1:10 in electrophoresis running buffer [25 mmol l⁻¹ Tris, 192 mmol l⁻¹ glycine, 0.1% (w/v) SDS], and 80 μl of each sample were applied to the system followed by repeated rinsing with transfer buffer (3×500 μl). A dilution series of pooled samples was used as a reference standard on each membrane (Fig. S3F), which were always loaded with randomly ordered samples from two egg batches (2×20 samples) yielding 12 runs in total (3×2 batches×4 proteins). After the loading process, membranes were immediately blocked for 1 h (RT) with TBS-T buffer containing 5% (w/v) non-fat skimmed milk powder. Methods for protein detection and imaging were the same as described above (see Antibody specificity). Signal intensity was analyzed using AIDA Image Analyzer software (version 3.52, Raytest, Straubenhardt, Germany). Values were recalculated from the reference curve and expressed as arbitrary units per mg protein content of the original sample (a.u. mg⁻¹ protein).

Immunolocalization of ion transport proteins

Fixed larvae (stage IV) were rehydrated in 0.1 mol l⁻¹ PBS (pH 7.4) and incubated for 30 min in 3% BSA to block non-specific binding during immunolocalization of NKA, ATP-synthase, VHA, NBC-1 and NKCC. Incubation with primary antibodies diluted 1:300 in PBS was done overnight at 2°C (see Table S2 for details on primary antibodies). After being carefully rinsed with PBS, larvae were

incubated for 2 h (RT) with two secondary antibodies (DyLight[®] 488 anti-mouse and DyLight[®] 594 anti-rabbit, Jackson ImmunoResearch, West Grove, PA, USA, diluted 1:300 in PBS) for co-localization of NBC1/NAK, NBC1/NKCC1, NBC1/ATP-synthase and NKA/VHA, respectively. Negative controls were performed for each pair without application of the primary antibody (Fig. S3G). Finally, larvae were rinsed once more with PBS and placed on a fluorescence slide prior to image acquisition with an inverse confocal laser-scanning microscope (Leica TCS SP5 II, Leica, Wetzlar, Germany). The total number of mitochondria (ATP-synthase)-rich ionocytes on the body surface of five larvae was evaluated using a cell-counter plugin for ImageJ[®] (ATCN 1.6). Ionocyte density was estimated from the number of cells divided by body area (cells mm⁻²).

Statistical analyses

Statistical analyses were conducted with the open source software R (www.r-project.org). If normality and homoscedasticity were not violated (assessed via Q–Q plots), linear mixed models (LME, package ‘lme4’; Bates et al., 2014) were applied (total mortality, enzyme activity-to-expression ratios). Otherwise, generalized linear mixed-effect models (GLMM, package ‘lme4’) were used (daily mortality, enzyme activity, protein expression) and appropriate probability distributions were assessed using the ‘MASS’ package (https://CRAN.R-project.org/package=MASS; Venables & Ripley, 2002). In all cases, different levels of temperature, P_{CO_2} and developmental stage were treated as fixed factors while egg batch was included as a random factor. The package ‘lsmeans’ (Lenth, 2016) with Tukey’s P -value corrections was used to conduct *post hoc* pairwise comparisons of single model factors. All data are presented as means (\pm s.e.m.) and statistical tests with $P < 0.05$ were considered significant. Statistical results are summarized in Table S3.

RESULTS

Fertilization and development times

The difference in mean (\pm s.e.m.) fertilization success under control conditions (88.4 \pm 4.3% at 6.0°C, 400 μ atm CO₂) and elevated P_{CO_2} (87.0 \pm 4.5% at 6.0°C, 1100 μ atm CO₂) was not significant (paired t -test, $P = 0.08$, $n = 6$). Temperature-dependent development times until stages I–V (Fig. 2A,B) were highly synchronous among egg batches (Fig. S2); differences between P_{CO_2} treatments were not detectable by visual inspection (data not shown).

Mortality

The influence of elevated P_{CO_2} on daily mortality rates of cod embryos was a function of incubation temperature and developmental stage (Fig. 2A,B), as indicated by an interaction between age, P_{CO_2} and temperature (GLMM: $P = 0.0233$). Increased mortality due to elevated P_{CO_2} occurred primarily during early development (cleavage and gastrulation, stages I–II) and in combination with warming. Few losses were observed during organogenesis, segmentation and hatching (stages II–IV). Total mortality until hatching (Fig. 2C) of embryos exposed to elevated P_{CO_2} and warming (28.2 \pm 0.5%) was 2-fold higher than in the control group (13.1 \pm 1.4%, *post hoc* test: $P < 0.0001$). Differences in mortality under either elevated P_{CO_2} (14.1 \pm 1.3%) or warming (16.1 \pm 1.2%) were not significant. These results clearly demonstrate that early embryogenesis (and particularly gastrulation) is a critical bottleneck with respect to the combined effects of elevated P_{CO_2} and temperature on Atlantic cod (Fig. 2D).

Enzyme activity

TA activity and specific activity of VHA, NKA and ATP-synthase increased with developmental stage in a similar, sigmoidal way in

all treatment combinations (GLMM, $P < 0.0001$; Fig. 3A,B). The activity of NKA, VHA and ATP-synthase was extremely low at stage I and II (end of gastrulation). Thereafter, activity increased exponentially until hatching (stage II–IV) while a less rapid increase was observed between hatching and yolk sac absorption (stage IV–V; Fig. 3B). Between the end of gastrulation and yolk sac absorption (stage II–V), enzyme specific activity increased 40- to 60-fold.

Incubation at elevated P_{CO_2} had no effect on TA activity (GLMM, $P = 0.145$), but caused a significant increase (20–30% at stage III–V) in the activity of NKA ($P = 0.021$), VHA ($P < 0.001$) and ATP-synthase ($P < 0.001$; Fig. 3B). Accordingly, there was a significant decrease in residual ATPase activity (the difference between TA activity and the sum of NKA, VHA and ATP-synthase activity) at elevated compared with control P_{CO_2} (GLMM, $P < 0.001$; Fig. 3D–G). The effect of elevated P_{CO_2} on enzyme activity (TA, NKA, VHA and ATP-synthase) did not differ between temperature treatments (Fig. 3A,B). In both CO₂ treatments, the summed contribution of NKA, VHA and ATP-synthase activity to TA activity decreased with warming, resulting in larger fractions of residual ATPase activity at 9.5°C compared with 6.5°C (GLMM, $P = 0.023$; Fig. 3D–G).

Protein expression

The protein expression of NKA, ATP-synthase and secondary ion transporters NKCC-1 and NBC1 (Fig. 4A–D) increased from low levels during cleavage and gastrulation (stage I and II) to a maximum at hatching (stage IV), followed by a 30–40% decrease during yolk sac absorption (GLMM, stage effect: $P < 0.001$). A trend towards increased protein expression at elevated P_{CO_2} was statistically not significant (Table S3). Incubation at increased temperature (9.5°C) led to an overall reduction in protein expression of ~40% (stage III–V) compared with that at 6.0°C (GLMM, $P < 0.05$).

Lower protein expression of NKA and ATP-synthase at 9.5°C compared with 6.0°C did not result in a difference in enzyme activity when assayed at a common temperature (Fig. 5A,B; Table S3). Moreover, enzyme activity of NKA and ATP-synthase increased throughout yolk sac absorption (stage V) despite a reduction in expression between stage IV and stage V (Fig. 5A,B). As a result, enzyme activity-to-expression ratios (indicating enzyme catalytic power) increased significantly due to warming and developmental progress (GLMM, $P < 0.0001$; Fig. 5C,D).

Ion transporter localization

All targeted ion transporters (NKA, VHA, NBC1 and NKCC1) and mitochondrial ATP-synthase were localized in epidermal ionocytes of newly hatched larvae (stage IV; Fig. 6A–F). Ionocytes located on the yolk sac and trunk were larger (~50 μ m diameter, Type I) than densely clustered ionocytes (~30 μ m, Type II) within the primordial gill cavity (Fig. 6A, top). Ionocyte density on the yolk sac ranged between 200 and 300 cells mm⁻², while more than 1000 cells mm⁻² were counted within the gill cavity (Fig. 6G). NBC1 was also localized around the apical pit of mucous cells (Fig. 6A,B), which occur across the entire body surface (see Ottesen and Olafsen, 1997). Immunoreactivity of adhesive mucous droplets (Fig. 6A, bottom) was probably caused by non-specific binding of antibodies.

DISCUSSION

Embryonic life stages are considered particularly vulnerable to environmental factors because of a lack of adult-like organ systems and associated capacity for homeostatic regulation (Hamdoun and

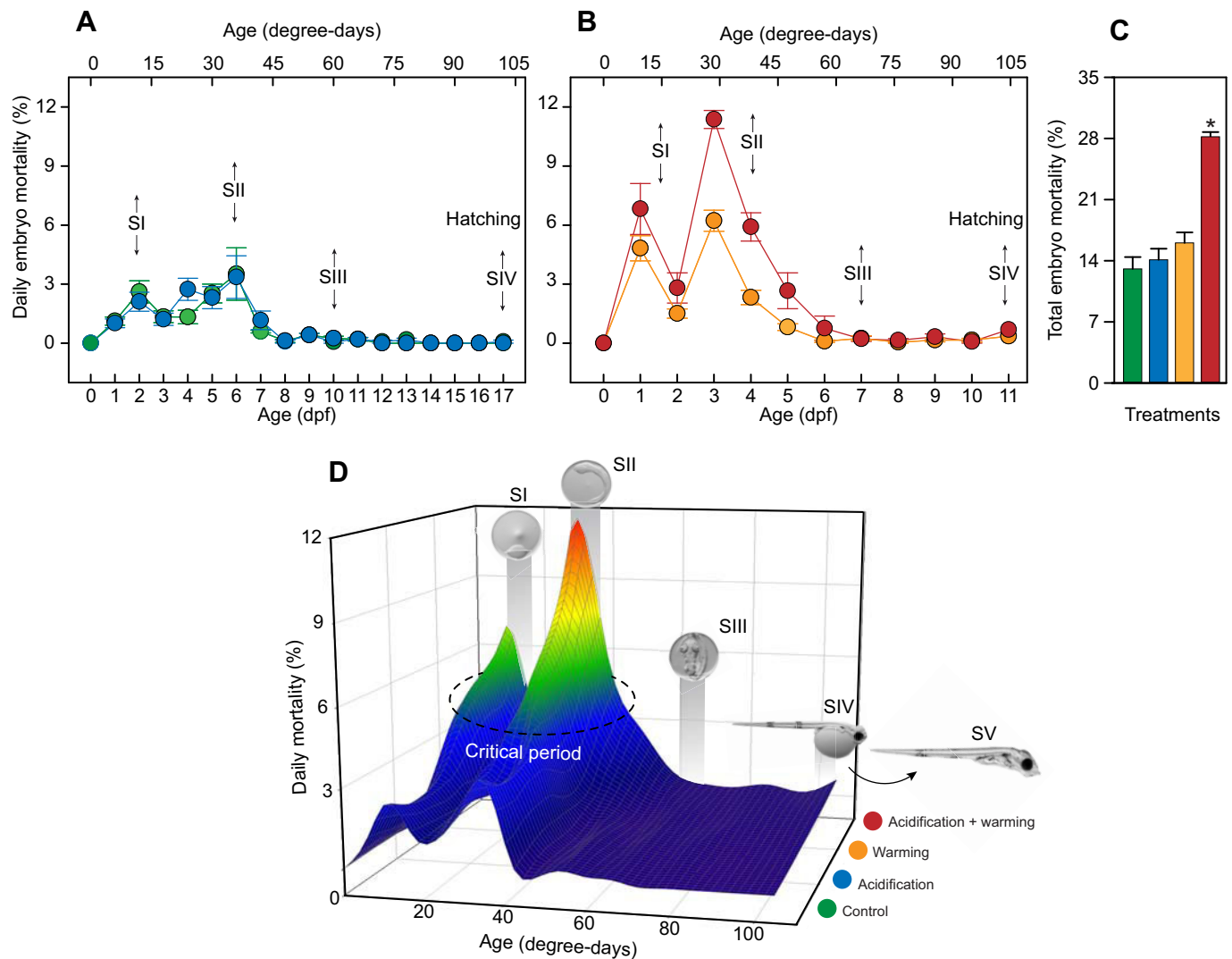


Fig. 2. Embryo mortality. (A,B) Stage-specific vulnerability of Atlantic cod embryos to ocean acidification and warming, assessed based on daily mortality rates (colored symbols, see D for color code) between fertilization and hatching (stage IV). Temperature-dependent development times until stages (S)I–IV (arrows) were normalized by means of degree-days (days post-fertilization \times incubation temperature, upper x-axis). dpf, days post-fertilization. (C) Total embryo mortality until hatching. Asterisk indicates significant treatment effects (least-square *post hoc* test with Tukey correction, $P < 0.05$). All values are given as means \pm s.e.m. ($n = 6$). (D) Three-dimensional representation of the relationship between embryo mortality, treatment combination and normalized developmental age (degree-days). Colored planes denote average mortality rates (as displayed in A and B). Images and gray shading indicate developmental times until stages I (late blastula), II (100% epiboly), III (50% eye pigmentation) and IV (hatching). Mortality was not assessed between hatching and yolk sac absorption (stage V), while all stages were sampled for analyses of enzyme activity and protein expression. High embryo vulnerability (mortality) to combined effects of elevated temperature and P_{CO_2} during gastrulation (stages I–II) identifies this period as particularly critical.

Epel, 2007; Melzner et al., 2009b). In line with this hypothesis, we found that Atlantic cod embryos are most vulnerable to the combined effects of ocean acidification and warming during early development, especially during gastrulation. The extremely low capacity for homeostatic regulation (activity and expression of ion transporters) throughout cleavage and gastrulation suggests that early embryogenesis is mainly protected by inherited (maternal) defense mechanisms. By the time of hatching, however, cod larvae were less sensitive and had ion transport and ATP production capacities similar to those of specialized adult gill tissue. Moreover, enhanced enzyme activity and modulation of protein expression levels in response to acidification and warming imply that post-gastrulation stages are increasingly capable of responding to changing environments via plasticity in the development of homeostatic mechanisms. Based on these results, a conceptual

model of fish early-life vulnerability and homeostatic plasticity is proposed in Fig. 7.

The combined effects of future ocean acidification and warming on offspring survival demonstrated in this study are consistent with previous work on Atlantic cod (Dahlke et al., 2017, 2018), Antarctic dragon fish *Gymnodraco acuticeps* (Flynn et al., 2015), sand lance *Ammodytes dubius* (Murray et al., 2019) and many other marine organisms (Przeslawski et al., 2015). Collectively, these data point to considerable risks for marine species and ecosystems if CO_2 emissions continue to rise over the coming decades (Hoegh-Guldberg et al., 2018). It should be noted, however, that our approach did not account for the possibility that species could adapt to the expected long-term changes in acidity and temperature through selection and/or transgenerational plasticity, i.e. parental effects (Chevin et al., 2010; Burggren, 2018). Several studies have

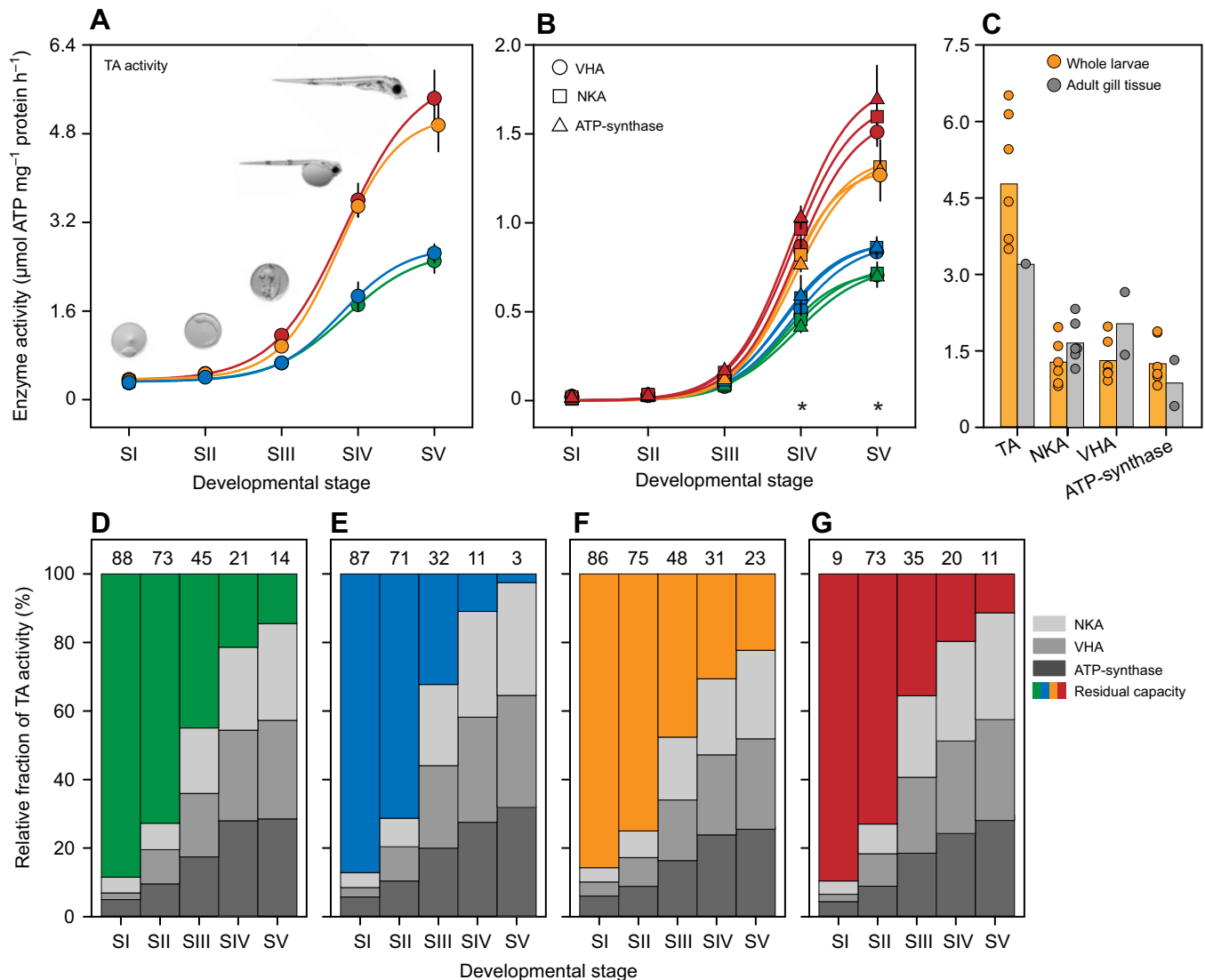


Fig. 3. Effects of elevated P_{CO_2} and temperature on the development of enzymatic ion transport capacity in Atlantic cod. (A) Total ATPase (TA) activity was determined to estimate (B) the specific activity of acid–base relevant ion pumps: V-type H^+ -ATPase (VHA), Na^+/K^+ -ATPase (NKA) and mitochondrial ATP-synthase at developmental stages I–V (images in A). See Fig. 1 for color code. Sigmoidal regressions (lines) illustrate response patterns. Asterisks indicate significant stage-specific CO_2 effects (averaged over temperature treatments, least-square contrast with Tukey correction, $P < 0.05$). (C) Activity of TA, VHA, NKA and ATP-synthase measured in cod larvae (stage V, 9.5°C assay temperature) and gill tissue of adult cod (10°C assay temperature; as reported by Kreiss et al., 2015; Melzner et al., 2009a; Michael et al., 2016a,b). All values are means \pm s.e.m. ($n=6$). (D–G) Stacked bar charts illustrating fractions of transporter-specific enzyme activity (NKA, VHA and ATP-synthase) and residual ATPase activity (colored fractions; numbers indicate percentages) relative to TA under different treatment conditions.

shown that parent–environment interactions, including epigenetic mechanisms, can alter offspring responses (reaction norms) to environmental factors (e.g. Dahlke et al., 2016; Shama et al., 2014; Schunter et al., 2018), potentially enabling physiological adaptation to moderate climate change (but see Byrne et al., 2019). However, phylogenetic analyses of past adaptation rates (Quintero and Wiens, 2013; Comte and Olden, 2017) and observed distribution shifts of marine species to higher latitudes and/or greater depths in response to global warming (Burrows et al., 2019; Pinsky et al., 2013) indicate that, for many species, adaptation of physiological thresholds may be too slow to keep pace with ongoing anthropogenic climate change (Hoegh-Guldberg et al., 2018). Our results primarily emphasize the importance of understanding the development of homeostatic capacity and associated lifecycle bottlenecks as a basis for reliable climate risk assessment.

Critical periods during development often coincide with functional transitions (Burggren and Mueller, 2015), such as those occurring during gastrulation. This early period is characterized by complex morphogenetic processes, including the maternal-to-zygotic transition (MZT), where developmental control is handed over from maternally provisioned factors (e.g. mRNAs, enzymes and chaperones) to those synthesized from the embryonic genome (Schier, 2007; Kimmel et al., 1995). Moreover, gastrulation leads to the formation of germ layers which give rise to different tissues and organ systems (Kimmel et al., 1995). Any defect at this stage may cause disproportionately serious damage, leading to either instantaneous mortality or deformities. In fact, high vulnerability of gastrula stages to diverse abiotic stressors (e.g. temperature, CO_2 , UV radiation, hypoxia or toxicants) was demonstrated in different gadoid species (Dahlke et al., 2017;

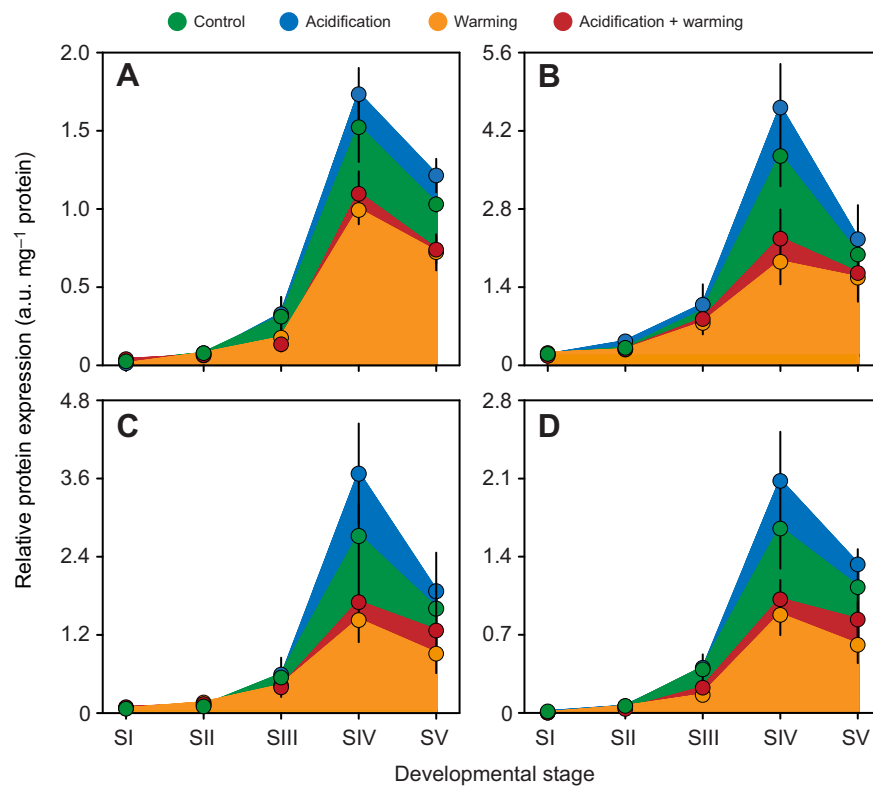


Fig. 4. Effects of acidification and warming on stage-specific expression of ion transporters during early development of Atlantic cod. Protein expression of (A) NKA, (B) ATP-synthase, (C) $\text{Na}^+/\text{K}^+/\text{2Cl}^-$ cotransporter 1 (NKCC1) and (D) $\text{Na}^+/\text{HCO}_3^-$ cotransporter 1 (NBC1), expressed as arbitrary units (a.u., means \pm s.e.m., $n=6$). Treatment conditions and developmental stages are shown in Fig. 1.

Kouwenberg et al., 1999; Nahrgang et al., 2017; Skjærven et al., 2013; Wieland et al., 1994), as well as in model organisms like zebrafish, *Danio rerio* (Ali et al., 2011; Jesuthasan and Strähle, 1997; Sawant et al., 2014), fruit fly, *Drosophila melanogaster* (Bergh and Arking, 1984), and clawed frog, *Xenopus laevis* (Heikkilä et al., 1985; Metikala et al., 2018; Degitz et al., 2000). Overall, these observations identify the gastrulation period as a critical lifecycle bottleneck for many, if not all, metazoans.

Proposed mechanisms underlying embryo mortality from external stressors include impairment of functions related to cell division and cell motility, such as pH-sensitive and energy-dependent microtubule dynamics (Cheng et al., 2004; Zalik et al., 1999). It is thus likely that the increasing capacity for pH and energy homeostasis caused the observed decrease in cod embryo vulnerability after gastrulation (Fig. 7), although additional mechanisms may have been involved. For instance, studies on vertebrate and invertebrate model organisms suggest that inducible heat shock responses and apoptotic pathways occur after MZT (Rupik et al., 2011; Hamdoun and Epel, 2007), possibly contributing to reduced stress sensitivity of post-gastrulation stages.

The capacity of fish embryos and larvae for homeostatic regulation is thought to be linked to the differentiation of extrabranchial (epidermal) ionocytes (Burggren and Bautista, 2019; Varsamos et al., 2005). Proportional changes in the expression and activity of primary (NKA, VHA) and secondary ion transporters (NBC1, NKCC1), as well as their localization in mitochondria (ATP-synthase)-rich ionocytes suggest that early larvae and adults utilize similar ion regulation mechanisms to defend pH homeostasis against respiratory and environmental acidosis (Fig. 6H). Notably, the high enzyme activity of cod larvae (whole-animal extracts, stage V) was similar to that in specialized adult gill tissue, indicating that these fragile life stages are already equipped with powerful homeostasis systems. From an evolutionary perspective, this appears plausible given that fish larvae are among

the fastest growing vertebrates ($30\% \text{ day}^{-1}$ in cod; Finn et al., 2002) with correspondingly high requirements for efficient removal of metabolic CO_2 and acid-base regulation (Brauner and Rombough, 2012). In fact, an early study (Ishimatsu et al., 2004) showed that (short-term) survival of marine fish larvae is possible at P_{CO_2} levels ($>10,000 \mu\text{atm}$) 10-fold higher than those projected for the end of this century.

While all investigated ion transporters are highly expressed by ionocytes of newly hatched cod larvae (Fig. 6), it was not possible to determine the contribution of these cells to whole-organism homeostatic capacity. However, observed changes in whole-organism enzyme activity and protein expression due to elevated P_{CO_2} and temperature are consistent with the idea that developmental (or homeostatic) plasticity allows species to maintain fitness within a limited range of environmental conditions (Burggren, 2018). Early mortality of embryos with insufficient homeostatic capacity (i.e. selection of beneficial genotypes) provides an alternative explanation for the observed treatment effects on NKA, VHA and ATP-synthase activity and expression. However, selection through treatment-related mortality would have narrowed the data frequency distribution (e.g. at elevated P_{CO_2} compared with control conditions), which was clearly not the case (Fig. S2,D).

Higher catalytic power of enzymes (Fig. 5) in combination with higher kinetic energy at warmer temperatures may support maintenance of ionic balance despite lower expression (and energy expenditure) of ion transporters (Fields et al., 2015; Somero, 1995). This view is supported by an inverse relationship between incubation temperature and ionocyte density previously demonstrated in cod larvae (Dahlke et al., 2017). At extreme temperatures, however, energetic benefits associated with warm temperature acclimation are increasingly outweighed by rising maintenance costs and constraints on mitochondrial energy production (Dahlke et al., 2017; Leo et al., 2018).

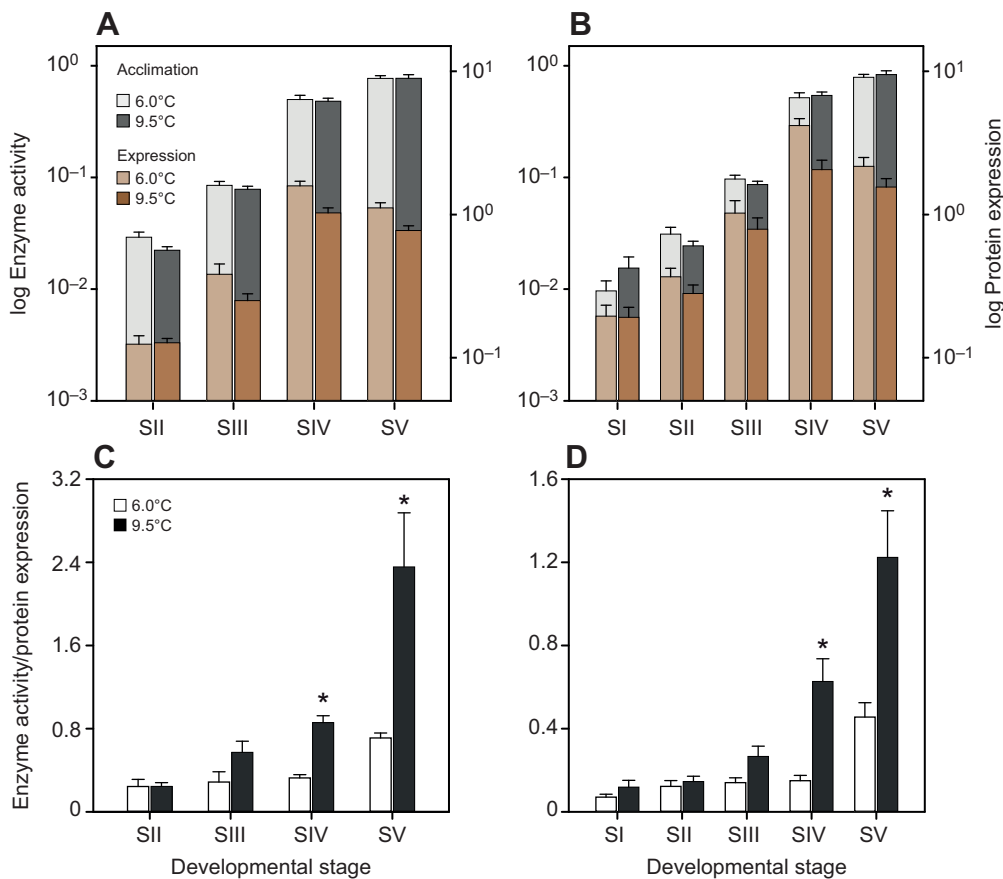


Fig. 5. Temperature effects on the relationship between enzyme activity and expression of NKA and mitochondrial ATP-synthase during early development of Atlantic cod. (A,B) Stage-specific ATP-synthase (A) and NKA (B) activity ($\mu\text{mol ATP h}^{-1} \text{mg}^{-1}$ protein; left y-axes) of embryos/larvae reared at 6.0°C (light gray) and 9.5°C (dark gray) was not significantly different when assayed at a common temperature (6.0°C, GLMM, $P>0.5$). The respective enzyme expression levels (a.u. mg^{-1} protein; right y-axes) of embryos/larvae reared at 6.0°C (light brown) and 9.5°C (dark brown) indicate lower expression levels at the higher temperature (GLMM, $P<0.05$). Means \pm s.e.m. ($n=12$, CO_2 treatments were pooled). (C,D) NKA (C) and ATP-synthase (D) activity-to-expression ratios determined at different stages for embryos incubated at 6.0°C (white) and 9.5°C (black). For NKA, stage I was excluded because of low expression levels. Asterisks indicate significant temperature effects at different stages (*post hoc* test, $P<0.05$).

Additional homeostatic requirements of cod embryos at elevated P_{CO_2} (1100 μatm) may have triggered the establishment of increased enzyme activity, as was previously demonstrated for gill NKA of adult cod (Melzner et al., 2009a) and eelpout *Zoaces viviparus* (Deigweier et al., 2008), although at much higher CO_2 concentrations (6000 and 10,000 μatm , respectively). Increased activity of VHA, NKA and ATP-synthase in cod embryos and larvae incubated at elevated P_{CO_2} implies that pH homeostasis and normal development under these conditions involves additional ATP-dependent ion transport in specialized ionocytes (Fig. 6H), but probably also in other cell types and tissues. Increased ATP demand by ionocytes under OA conditions may primarily relate to the activity of NKA, which facilitates electroneutral proton export via apical Na^+/H^+ exchanger (NHE) proteins, as well as bicarbonate buffering via basolateral NBC1 and NKCC1 by establishing and maintaining the required Na^+ and Cl^- gradient (Brauner et al., 2019; Fig. 6H). The observed increase in VHA activity may not be directly related to proton export by ionocytes, as our results and previous studies on marine fish do not provide evidence for an apical orientation of this transporter (Allmon and Esbaugh, 2017; Brauner et al., 2019). Instead, it is possible that the contribution of VHA to the maintenance of membrane potentials and various other cellular functions (e.g. acidification of lysosomes) (Tresguerres, 2016) led to an increased VHA activity and thus ATP demand at elevated P_{CO_2} .

In line with previous work on echinoderms (Pan et al., 2015), our results (e.g. smaller residual enzyme activity; Fig. 3D–G) indicate that additional costs for acid–base regulation and cellular maintenance at elevated P_{CO_2} are met through energy reallocation. In cod and many other fish species, altered energy budgets in

response to elevated P_{CO_2} are reflected by reductions in developmental growth (Cattano et al., 2018; Esbaugh, 2018; Dahlke et al., 2018), sometimes still detectable at the juvenile stage (Murray et al., 2016). Accordingly, our results link CO_2 -related enzyme adjustments with developmental trade-offs at the animal level (growth deficits), which in turn may contribute to increased susceptibility to natural sources of mortality, i.e. starvation and predation (Garrido et al., 2015).

Although it is clear that *in vitro* analyses of enzyme activity and expression cannot resolve the actual (*in vivo*) biochemical responses of an intact organism (Somero et al., 2017), we consider the presented data as reliable proxies. Firstly, the relative increase in total ATPase activity (*in vitro* metabolic capacity) between stage I and stage V is directly proportional to the increase in oxygen consumption (*in vivo* metabolic intensity) determined in cod embryos (Finn et al., 1995) over the same developmental period (Fig. S2,E). Secondly, the fractional activity of whole-larvae NKA (28.5% of TA activity at stage V) corresponds with the relative amount of available ATP (30%) that is typically allocated to regulate sodium–potassium fluxes in metabolically active tissues (Somero et al., 2017), including gill tissue (29–36%) of adult cod (Kreiss et al., 2015; Michael et al., 2016b).

Conclusion

A low capacity to maintain pH and energy homeostasis of early cod embryos corresponds with the concept (Fig. 7) that maternally provisioned defense mechanisms protect initial development against natural environmental variability (Hamdoun and Epel, 2007). Innate defense levels differ between locally adapted species or populations, sometimes due to parental pre-exposure (Byrne

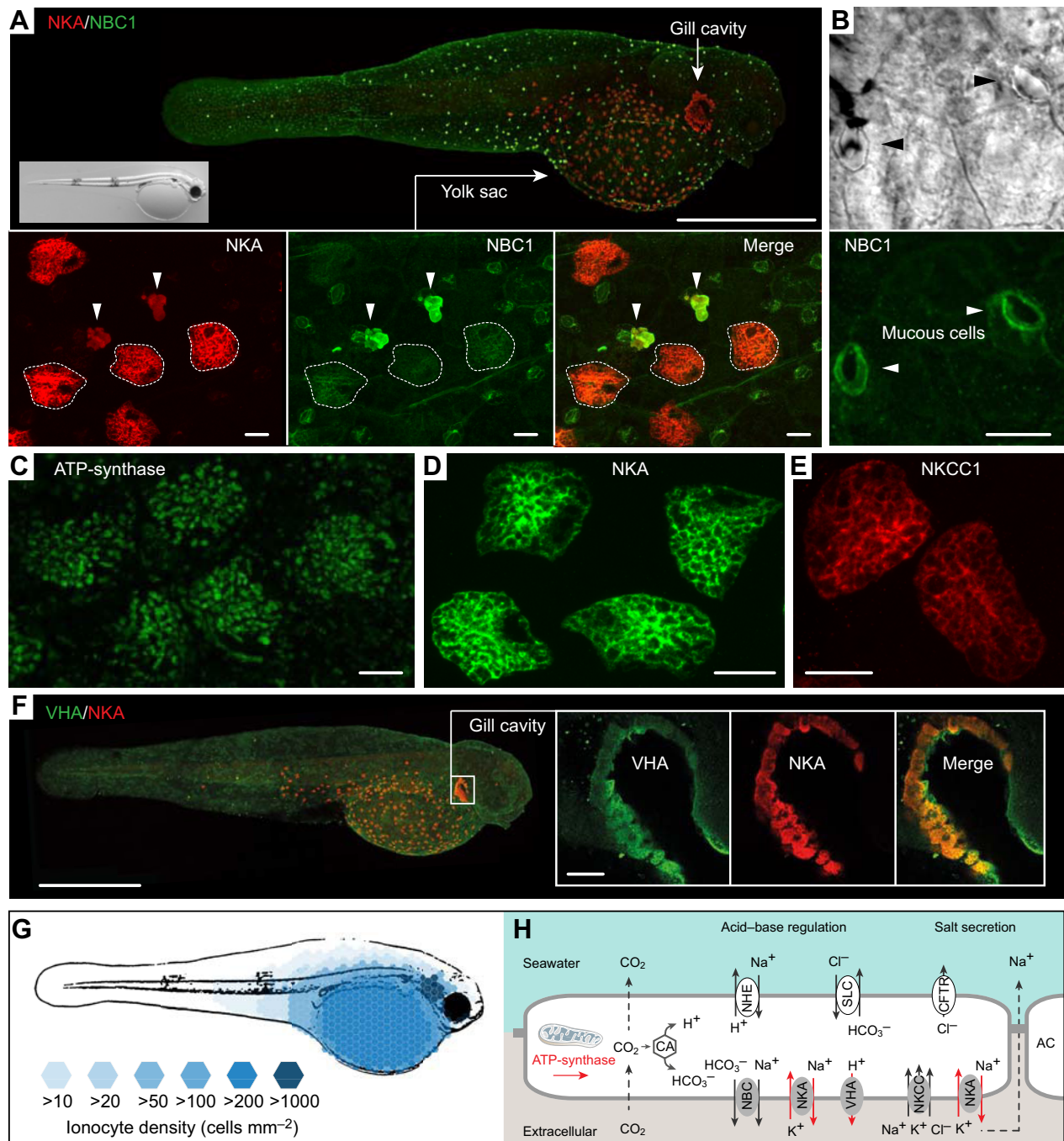


Fig. 6. Ion transporter localization. (A) Whole-mount confocal scan (top) and magnified sections (bottom) showing immunolocalization of NKA (red) and NBC1 (green) in a cod larva (stage IV, light image) reared under control conditions (6.0°C, 400 μatm CO₂). Orange indicates co-localization of the two transporters in ionocytes on the yolk sac (Type I, diameter ~50 μm) and within the gill cavity (Type II, diameter ~30 μm). Scale bar: 1 mm. The magnified sections show NKA/NBC1-positive ionocytes (stippled circles) on the yolk sac surrounded by smaller NBC1-positive mucous cells (green, magnified in B). Scale bars: 10 μm. (B) Light image (top) and confocal scan (bottom) showing NBC1-positive mucous cells (arrowheads). Scale bar: 10 μm. (C–E) Expression of ATP-synthase (C), NKA (D) and NKCC1 (E) by yolk sac ionocytes. Scale bars: 20 μm. (F) Orange indicates co-localization of VHA (green) and NKA (red) in ionocytes on the yolk sac and within the gill cavity. Scale bar: 1 mm. Inset: magnified sections of Type II ionocytes in the gill cavity. Scale bar: 20 μm. (G) Ionocyte density (colors are interpolated values, n=5 individuals) on the body surface of cod larvae reared under control conditions. (H) Hypothesized mechanisms of acid–base regulation and salt secretion by ionocytes of marine fish (reviewed by Evans et al., 2005; Brauner et al., 2019). Compensation of CO₂-induced acidosis involves hydration of CO₂ by carbonic anhydrase (CA) while the resulting protons (H⁺) are excreted across the apical membrane via Na⁺/H⁺ co-transporter (NHE). Excess bicarbonate (HCO₃⁻) ions are moved across the basolateral membrane by NBC1 to restore extracellular pH. Conversely, compensation of alkalosis occurs through apical export of bicarbonate via anion exchangers and basolateral transport of [H⁺] by VHA. Salt (NaCl) secretion involves basolateral import of Na⁺, K⁺ and Cl⁻ via NKCC1, apical export of Cl⁻ via cystic fibrosis transmembrane conductance regulator (CFTR), and paracellular exit of Na⁺ between accessory cells (AC) according to the electrochemical gradient maintained by basolateral NKA. In contrast to ATP-synthase, NKA, VHA, NBC1 and NKCC1 expression (gray), expression of CA, NHA, AE and CFTR (white) was not confirmed in this study. Red arrows indicate ATP-dependent ion transport processes.

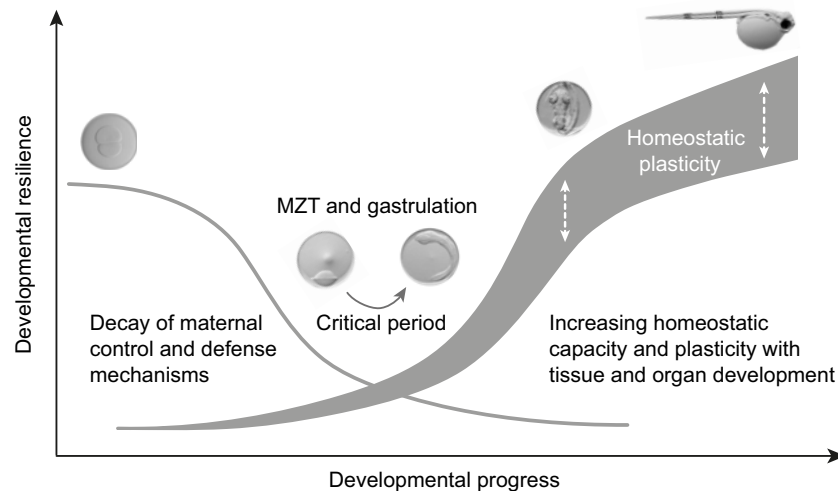


Fig. 7. Conceptual diagram of fish embryo vulnerability and homeostatic plasticity in a climate change context. Early embryogenesis is controlled and protected by provisioned (innate) factors (e.g. maternal mRNAs and chaperones), which buffer developmental processes against expected environmental conditions before regulatory defenses, including ion transport mechanisms, are sufficiently effective (Hamdoun and Epel, 2007). The progressive decay of innate defense factors between fertilization and the maternal–zygotic transition (MZT) (Tadros and Lipshitz, 2009) is paralleled by a rise in the capacity for homeostatic regulation. High vulnerability during the MZT and gastrulation probably results from the coincidence of low homeostatic capacity and the inherent instability of developmental processes during this particularly critical period (Jesuthasan and Strähle, 1997). Increased tolerance of later stages is associated with the differentiation of organs and specialized cells (e.g. ionocytes) in combination with the establishment of heat-shock responses (Rupik et al., 2011) and the ability to adjust homeostatic capacity via changes in gene expression (Scott et al., 2012). Plasticity of homeostasis functions can facilitate short-term acclimatization to environmental change, although such responses are often associated with energetic trade-offs.

et al., 2019). Future climate changes may exceed the range of natural variability and thus innate defense levels. The establishment of improved tolerance after the critical gastrulation period most likely involves increasing capacity for homeostatic regulation associated with the differentiation of specialized cells (ionocytes) and organ systems (Varsamos et al., 2005). Regulatory mechanisms of early cod larvae are more sophisticated than previously expected, possibly reflecting a physiological prerequisite for highly active and rapidly growing fish larvae (Rombough, 2011). Capacity adjustments and modifications of regulatory mechanisms potentially support short-term (within-generation) acclimatization to environmental change, but the extent of homeostatic plasticity may cause additional energetic costs and trade-offs.

Acknowledgements

We acknowledge the technical support of Silvia Hardenberg, Elettra Leo, Felix Mark, Martina Stiasny, Catriona Clemmensen and Gwendolin Göttler. Special thanks are dedicated to the staff of the Tromsø Aquaculture Research Station and the Centre for Marine Aquaculture.

Competing interests

The authors declare no competing or financial interests.

Author contributions

Conceptualization: F.D., H.-O.P., D.S.; Methodology: F.D., M.L., U.B.; Formal analysis: F.D., S.W., M.C.; Investigation: F.D.; Resources: M.L., U.B., A.M., V.P.; Writing - original draft: F.D.; Writing - review & editing: F.D., M.L., U.B., S.W., H.-O.P., D.S.; Visualization: F.D.; Supervision: H.-O.P., D.S.; Funding acquisition: H.-O.P., D.S.

Funding

Funding was received from the research program BIOACID (Biological Impacts of Ocean Acidification) by the German Federal Ministry of Education and Research (Bundesministerium für Bildung und Forschung: FKZ 03F0655B and FKZ 03F0728B). Funding was also received from AQUAEXCEL (AQUAculture infrastructures for EXCELlence in European fish research; TNA 0092/06/08/21 to D.S.). F.D., M.L., U.B., H.-O.P. and D.S. were supported by the PACES (Polar Regions and Coasts in a Changing Earth System) program of the Alfred Wegener Institute Helmholtz Centre for Polar and Marine Research (AWI). S.W. was

supported by the Helmholtz Institute for Functional Marine Biodiversity (HIFMB), which is a collaboration between the AWI and the Carl-von-Ossietzky University Oldenburg, initially funded by the Ministry for Science and Culture of Lower Saxony and the Volkswagen Foundation through the 'Niedersächsisches Vorab' grant program (grant ZN3285).

Supplementary information

Supplementary information available online at <http://jeb.biologists.org/lookup/doi/10.1242/jeb.212589.supplemental>

References

- Alderdice, D. (1988). 3 Osmotic and ionic regulation in teleost eggs and larvae. *Fish Physiol.* **11**, 163–251. doi:10.1016/S1546-5098(08)60200-9
- Ali, S., Champagne, D. L., Alia, A. and Richardson, M. K. (2011). Large-scale analysis of acute ethanol exposure in zebrafish development: a critical time window and resilience. *PLoS ONE* **6**, e20037. doi:10.1371/journal.pone.0020037
- Allmon, E. B. and Esbaugh, A. J. (2017). Carbon dioxide induced plasticity of branchial acid-base pathways in an estuarine teleost. *Sci. Rep.* **7**, 45680. doi:10.1038/srep45680
- Bates, D., Mächler, M., Bolker, B. and Walker, S. (2014). Fitting linear mixed-effects models using lme4. *J. Stat. Soft.* **67**. doi:10.18637/jss.v067.i01
- Bergh, S. and Arking, R. (1984). Developmental profile of the heat shock response in early embryos of *Drosophila*. *J. Exp. Zool.* **231**, 379–391. doi:10.1002/jez.1402310312
- Bradford, M. M. (1976). Rapid and sensitive method for quantitation of microgram quantities of protein utilizing principle of protein-dye binding. *Anal. Biochem.* **72**, 248–254. doi:10.1016/0003-2697(76)90527-3
- Brauner, C. J. and Rombough, P. J. (2012). Ontogeny and paleophysiology of the gill: new insights from larval and air-breathing fish. *Respir. Physiol. Neurobiol.* **184**, 293–300. doi:10.1016/j.resp.2012.07.011
- Brauner, C. J., Shartau, R. B., Damsgaard, C., Esbaugh, A. J., Wilson, R. W. and Grosell, M. (2019). Acid-base physiology and CO₂ homeostasis: regulation and compensation in response to elevated environmental CO₂. *Fish Physiol.* **37**, 69–132. doi:10.1016/bs.fp.2019.08.003
- Brown, J. A., Minkoff, G. and Puvanendran, V. (2003). Larviculture of Atlantic cod (*Gadus morhua*): progress, protocols and problems. *Aquaculture* **227**, 357–372. doi:10.1016/S0044-8486(03)00514-3
- Burggren, W. (2018). Developmental phenotypic plasticity helps bridge stochastic weather events associated with climate change. *J. Exp. Biol.* **221**, jeb161984. doi:10.1242/jeb.161984
- Burggren, W. and Bautista, N. (2019). Invited review: Development of acid-base regulation in vertebrates. *Comp. Biochem. Physiol. A Mol. Integr. Physiol.* **236**, 110518. doi:10.1016/j.cbpa.2019.06.018

- Burggren, W. W. and Mueller, C. A.** (2015). Developmental critical windows and sensitive periods as three-dimensional constructs in time and space. *Physiol. Biochem. Zool.* **88**, 91-102. doi:10.1086/679906
- Burrows, M. T., Bates, A. E., Costello, M. J., Edwards, M., Edgar, G. J., Fox, C. J., Halpern, B. S., Hiddink, J. G., Pinsky, M. L. and Batt, R. D.** (2019). Ocean community warming responses explained by thermal affinities and temperature gradients. *Nat. Clim. Chang.* **9**, 959-963. doi:10.1038/s41558-019-0631-5
- Byrne, M., Foo, S. A., Ross, P. M. and Putnam, H. M.** (2019). Limitations of cross- and multigenerational plasticity for marine invertebrates faced with global climate change. *Glob. Change Biol.* **26**, 80-102. doi:10.1111/gcb.14882
- Cattano, C., Claudet, J., Domenici, P. and Milazzo, M. J. E. M.** (2018). Living in a high CO₂ world: A global meta-analysis shows multiple trait-mediated fish responses to ocean acidification. *Ecol. Monogr.* **88**, 320-335. doi:10.1002/ecm.1297
- Cheng, J. C., Miller, A. L. and Webb, S. E.** (2004). Organization and function of microfilaments during late epiboly in zebrafish embryos. *Dev. Dyn.* **231**, 313-323. doi:10.1002/dvdy.20144
- Chevin, L.-M., Lande, R. and Mace, G. M.** (2010). Adaptation, plasticity, and extinction in a changing environment: towards a predictive theory. *PLoS Biol.* **8**, e1000357. doi:10.1371/journal.pbio.1000357
- Comte, L. and Olden, J. D.** (2017). Climatic vulnerability of the world's freshwater and marine fishes. *Nat. Clim. Chang.* **7**, nclimate3382. doi:10.1038/nclimate3382
- Dahlke, F. T., Politis, S. N., Butts, I., Trippel, E. A., Peck, M. and Ecology** (2016). Fathers modify thermal reaction norms for hatching success in Atlantic cod, *Gadus morhua*. *J. Exp. Mar. Biol. Ecol.* **474**, 148-155. doi:10.1016/j.jembe.2015.10.008
- Dahlke, F. T., Leo, E., Mark, F. C., Portner, H. O., Bickmeyer, U., Frickenhaus, S. and Storch, D.** (2017). Effects of ocean acidification increase embryonic sensitivity to thermal extremes in Atlantic cod, *Gadus morhua*. *Glob. Change Biol.* **23**, 1499-1510. doi:10.1111/gcb.13527
- Dahlke, F. T., Butzin, M., Nahrgang, J., Puvanendran, V., Mortensen, A., Portner, H. O. and Storch, D.** (2018). Northern cod species face spawning habitat losses if global warming exceeds 1.5°C. *Sci. Adv.* **4**. doi:10.1126/sciadv.aas8821
- Degitz, S. J., Kosian, P. A., Makynen, E. A., Jensen, K. M. and Ankley, G. T.** (2000). Stage- and species-specific developmental toxicity of all-trans retinoic acid in four native North American ranids and *Xenopus laevis*. *Toxicol. Sci.* **57**, 264-274. doi:10.1093/toxsci/57.2.264
- Deigweier, K., Koschnick, N., Portner, H. O. and Lucassen, M.** (2008). Acclimation of ion regulatory capacities in gills of marine fish under environmental hypercapnia. *Am. J. Physiol. Regul. Integr. Comp. Physiol.* **295**, R1660-R1670. doi:10.1152/ajpregu.90403.2008
- Dickson, A. G., Sabine, C. L. and Christian, J. R.** (eds). (2007). Guide to best practices for ocean CO₂ measurements. *PICES special publication* 3, 191 pp.
- Esbaugh, A. J.** (2018). Physiological implications of ocean acidification for marine fish: emerging patterns and new insights. *J. Comp. Physiol. B – Biochem. Syst. Envir. Physiol.* **188**, 1-13. doi:10.1007/s00360-017-1105-6
- Evans, D. H., Piermarini, P. M. and Choe, K. P.** (2005). The multifunctional fish gill: Dominant site of gas exchange, osmoregulation, acid-base regulation, and excretion of nitrogenous waste. *Physiol. Rev.* **85**, 97-177. doi:10.1152/physrev.00050.2003
- Fields, P. A., Dong, Y. W., Meng, X. L. and Somero, G. N.** (2015). Adaptations of protein structure and function to temperature: there is more than one way to 'skin a cat'. *J. Exp. Biol.* **218**, 1801-1811. doi:10.1242/jeb.114298
- Finn, R. N. and Kapoor, B.** (2008). *Fish Larval Physiology*. Science Publishers, Inc.
- Finn, R. N., Fyhn, H. J. and Evjen, M. S.** (1995). Physiological energetics of developing embryos and yolk-sac larvae of Atlantic cod (*Gadus morhua*) .1. Respiration and nitrogen metabolism. *Mar. Biol.* **124**, 355-369.
- Finn, R. N., Rønnestad, I., Van Der Meeren, T. and Fyhn, H. J.** (2002). Fuel and metabolic scaling during the early life stages of Atlantic cod *Gadus morhua*. *Mar. Ecol. Prog. Ser.* **243**, 217-234. doi:10.3354/meps243217
- Flynn, E. E., Bjelde, B. E., Miller, N. A. and Todgham, A. E.** (2015). Ocean acidification exerts negative effects during warming conditions in a developing Antarctic fish. *Conserv. Physiol.* **3**, 355-369. doi:10.1007/BF00363909
- Garrido, S., Ben-Hamadou, R., Santos, A., Ferreira, S., Teodósio, M., Cotano, U., Irigoien, X., Peck, M., Saiz, E. and Ré, P.** (2015). Born small, die young: Intrinsic, size-selective mortality in marine larval fish. *Sci. Rep.* **5**, 17065. doi:10.1038/srep17065
- Hall, T. E., Smith, P. and Johnston, I. A.** (2004). Stages of embryonic development in the Atlantic cod *Gadus morhua*. *J. Morphol.* **259**, 255-270. doi:10.1002/jmor.10222
- Hamdoun, A. and Epel, D.** (2007). Embryo stability and vulnerability in an always changing world. *Proc. Natl Acad. Sci. USA* **104**, 1745-1750. doi:10.1073/pnas.0610108104
- Heikkilä, J. J., Kloc, M., Bury, J., Schultz, G. A. and Browder, L. W.** (1985). Acquisition of the heat-shock response and thermotolerance during early development of *Xenopus laevis*. *Dev. Biol.* **107**, 483-489. doi:10.1016/0012-1606(85)90329-X
- Hoegh-Guldberg, O., Jacob, D., Taylor, M., Bindi, M., Brown, S., Camilloni, I., Diedhiou, A., Djalante, R., Ebi, K. L. and Engelbrecht, F.** (2018). Impacts of 1.5°C global warming on natural and human systems. *Global Warming of 1.5°C: An IPCC Special Report on the impacts of global warming of 1.5°C above pre-industrial levels and related global greenhouse gas emission pathways, in the context of strengthening the global response to the threat of climate change, sustainable development, and efforts to eradicate poverty.* IPCC.
- IPCC** (2019). Summary for policymakers. In *IPCC's Special Report on the Ocean and Cryosphere in a Changing Climate* (ed. H.-O. Pörtner, D. C. R.V., Masson-Delmotte, P. Zhai, M., Tignor, E., Poloczanska, K., Mintenbeck, A., Alegría, M. Nicolai, A. Okem, J. Petzold, B. Rama and N. M. Weyer). In press.
- Ishimatsu, A., Kikkawa, T., Hayashi, M., Lee, K.-S. and Kita, J.** (2004). Effects of CO₂ on marine fish: larvae and adults. *J. Oceanography* **60**, 731-741. doi:10.1007/s10872-004-5765-y
- Jesuthasan, S. and Strähle, U.** (1997). Dynamic microtubules and specification of the zebrafish embryonic axis. *Curr. Biol.* **7**, 31-42. doi:10.1016/S0960-9822(06)00025-X
- Kimmel, C. B., Ballard, W. W., Kimmel, S. R., Ullmann, B. and Schilling, T. F.** (1995). Stages of embryonic development of the zebrafish. *Dev. Dyn.* **203**, 253-310. doi:10.1002/aja.1002030302
- Kouwenberg, J., Browman, H., Cullen, J., Davis, R., St-Pierre, J.-F. and Runge, J.** (1999). Biological weighting of ultraviolet (280–400 nm) induced mortality in marine zooplankton and fish. I. Atlantic cod (*Gadus morhua*) eggs. *Mar. Biol.* **134**, 269-284. doi:10.1007/s002270050545
- Kreiss, C. M., Michael, K., Bock, C., Lucassen, M. and Portner, H. O.** (2015). Impact of long-term moderate hypercapnia and elevated temperature on the energy budget of isolated gills of Atlantic cod (*Gadus morhua*). *Comp. Biochem. Physiol. A Mol. Integr. Physiol.* **182**, 102-112. doi:10.1016/j.cbpa.2014.12.019
- Laemmli, U. K.** (1970). Cleavage of structural proteins during assembly of head of bacteriophage-T4. *Nature* **227**, 680-685. doi:10.1038/227680a0
- Lenth, R. V.** (2016). Least-squares means: the R package lsmeans. *J. Stat. Softw.* **69**, 1-33. doi:10.18637/jss.v069.i01
- Leo, E., Dahlke, F. T., Storch, D., Pörtner, H.-O. and Mark, F. C.** (2018). Impact of Ocean Acidification and Warming on the bioenergetics of developing eggs of Atlantic herring *Clupea harengus*. *Conser. Physiol.* **6**, coy050. doi:10.1093/conphys/coy050
- Lewis, E., Wallace, D. and Allison, L. J.** (1998). Program developed for CO₂ system calculations. Brookhaven National Lab., Dept. of Applied Science, Upton, NY (United States); Oak Ridge National Lab., Carbon Dioxide Information Analysis Center, TN (United States).
- Melzner, F., Gobel, S., Langenbuch, M., Gutowska, M. A., Portner, H. O. and Lucassen, M.** (2009a). Swimming performance in Atlantic Cod (*Gadus morhua*) following long-term (4-12 months) acclimation to elevated seawater P-CO₂. *Aquat. Toxicol.* **92**, 30-37. doi:10.1016/j.aquatox.2008.12.011
- Melzner, F., Gutowska, M. A., Langenbuch, M., Dupont, S., Lucassen, M., Thorndyke, M. C., Bleich, M. and Portner, H. O.** (2009b). Physiological basis for high CO₂ tolerance in marine ectothermic animals: pre-adaptation through lifestyle and ontogeny? *Biogeosciences* **6**, 2313-2331. doi:10.5194/bg-6-2313-2009
- Metikala, S., Neuhaus, H. and Hollemann, T.** (2018). A multichannel computer-driven system to raise aquatic embryos under selectable hypoxic conditions. *Hypoxia* **6**, 1. doi:10.2147/HP.S151536
- Michael, K., Koschnick, N., Pörtner, H.-O. and Lucassen, M.** (2016a). Response of branchial Na⁺/K⁺ ATPase to changes in ambient temperature in Atlantic cod (*Gadus morhua*) and whiting (*Merlangius merlangus*). *J. Comp. Physiol. B Biochem. Syst. Envir. Physiol.* **186**, 461-470. doi:10.1007/s00360-016-0970-8
- Michael, K., Kreiss, C. M., Hu, M. Y., Koschnick, N., Bickmeyer, U., Dupont, S., Portner, H. O. and Lucassen, M.** (2016b). Adjustments of molecular key components of branchial ion and pH regulation in Atlantic cod (*Gadus morhua*) in response to ocean acidification and warming. *Comp. Biochem. Physiol. B Biochem. Mol. Biol.* **193**, 33-46. doi:10.1016/j.cbpb.2015.12.006
- Murray, C. S., Fuiman, L. A., Baumann, H. and Browman, H. E. H.** (2016). Consequences of elevated CO₂ exposure across multiple life stages in a coastal forage fish. *ICES J. Mar. Sci.* **74**, 1051-1061. doi:10.1093/icesjms/fsw179
- Murray, C. S., Wiley, D. and Baumann, H.** (2019). High sensitivity of a keystone forage fish to elevated CO₂ and temperature. *Conser. Physiol.* **7**, coz084. doi:10.1093/conphys/coz084
- Nahrgang, J., Dubourg, P., Frantzen, M., Storch, D., Dahlke, F. and Meador, J. P.** (2017). "Early life stages of an arctic keystone species (*Boreogadus saida*) show high sensitivity to a water-soluble fraction of crude oil" (vol 218, pg 605, 2016). *Environ. Pollut.* **223**, 120-120. doi:10.1016/j.envpol.2016.12.062
- Ottesen, O. and Olafsen, J.** (1997). Ontogenetic development and composition of the mucous cells and the occurrence of saccular cells in the epidermis of Atlantic halibut. *J. Fish Biol.* **50**, 620-633. doi:10.1111/j.1095-8649.1997.tb01954.x
- Pan, T.-C. F., Applebaum, S. L. and Manahan, D. T.** (2015). Experimental ocean acidification alters the allocation of metabolic energy. *Proc. Natl. Acad. Sci. USA* **112**, 4696-4701. doi:10.1073/pnas.1416967112
- Pinsky, M. L., Worm, B., Fogarty, M. J., Sarmiento, J. L. and Levin, S. A.** (2013). Marine taxa track local climate velocities. *Science* **341**, 1239-1242. doi:10.1126/science.1239352
- Pörtner, H.-O.** (2008). Ecosystem effects of ocean acidification in times of ocean warming: a physiologist's view. *Mar. Ecol. Prog. Ser.* **373**, 203-217. doi:10.3354/meps07768

- Przeslawski, R., Byrne, M. and Mellin, C. (2015). A review and meta-analysis of the effects of multiple abiotic stressors on marine embryos and larvae. *Glob. Change Biol.* **21**, 2122-2140. doi:10.1111/gcb.12833
- Puvanendran, V., Falk-Petersen, I. B., Lysne, H., Tveiten, H., Toften, H. and Peruzzi, S. (2015). Effects of different step-wise temperature increment regimes during egg incubation of Atlantic cod (*Gadus morhua* L.) on egg viability and newly hatched larval quality. *Aquac. Res.* **46**, 226-235. doi:10.1111/are.12173
- Quintero, I. and Wiens, J. J. (2013). Rates of projected climate change dramatically exceed past rates of climatic niche evolution among vertebrate species. *Ecol. Lett.* **16**, 1095-1103. doi:10.1111/ele.12144
- Rombough, P. (2011). The energetics of embryonic growth. *Respir. Physiol. Neurobiol.* **178**, 22-29. doi:10.1016/j.resp.2011.04.026
- Rombough, P. J. (1997). *The effects of temperature on embryonic and larval development. Seminar Series-Society For Experimental Biology*, pp. 177-224. Cambridge University Press.
- Rupik, W., Jasik, K., Bembenek, J. and Widlak, W. (2011). The expression patterns of heat shock genes and proteins and their role during vertebrate's development. *Comp. Biochem. Physiol. A Mol. Integr. Physiol.* **159**, 349-366. doi:10.1016/j.cbpa.2011.04.002
- Sawant, P. B., Bera, A., Dasgupta, S., Sawant, B. T., Chadha, N. K. and Pal, A. K. (2014). p53 dependent apoptotic cell death induces embryonic malformation in *Carassius auratus* under chronic hypoxia. *PLoS ONE* **9**, e102650. doi:10.1371/journal.pone.0102650
- Schier, A. F. (2007). The maternal-zygotic transition: death and birth of RNAs. *Science* **316**, 406-407. doi:10.1126/science.1140693
- Schnurr, M. E., Yin, Y. and Scott, G. R. (2014). Temperature during embryonic development has persistent effects on metabolic enzymes in the muscle of zebrafish. *J. Exp. Biol.* **217**, 1370-1380. doi:10.1242/jeb.094037
- Schunter, C., Welch, M. J., Nilsson, G. E., Rummer, J. L., Munday, P. L., Ravasi, T. J. N. E. and Evolution (2018). An interplay between plasticity and parental phenotype determines impacts of ocean acidification on a reef fish. *Nat. Ecol. Evol.* **2**, 334-342. doi:10.1038/s41559-017-0428-8
- Scott, G. R., Schnurr, M. E., Yin, Y. and Johnston, I. A. (2012). Embryonic temperature produces persistent effects on the capacity for thermal acclimation in adult zebrafish. *Proc. Natl Acad. Sci. USA*.
- Scott, J. D., Alexander, M. A., Murray, D. R., Swales, D. and Eischeid, J. (2016). The climate change web portal: A system to access and display climate and Earth system model output from the CMIP5 archive. *Bull. Am. Meteorol. Soc.* **97**, 523-530. doi:10.1175/BAMS-D-15-00035.1
- Shama, L. N., Strobel, A., Mark, F. C. and Wegner, K. M. (2014). Transgenerational plasticity in marine sticklebacks: maternal effects mediate impacts of a warming ocean. *Funct. Ecol.* **28**, 1482-1493. doi:10.1111/1365-2435.12280
- Skjærven, K. H., Penglase, S., Olsvik, P. A. and Hamre, K. (2013). Redox regulation in Atlantic cod (*Gadus morhua*) embryos developing under normal and heat-stressed conditions. *Free Radic. Biol. Med.* **57**, 29-38. doi:10.1016/j.freeradbiomed.2012.11.022
- Sokolova, I. M., Frederich, M., Bagwe, R., Lannig, G. and Sukhotin, A. A. (2012). Energy homeostasis as an integrative tool for assessing limits of environmental stress tolerance in aquatic invertebrates. *Mar. Environ. Res.* **79**, 1-15. doi:10.1016/j.marenvres.2012.04.003
- Somero, G. N. (1995). Proteins and temperature. *Annu. Rev. Physiol.* **57**, 43-68. doi:10.1146/annurev.ph.57.030195.000355
- Somero, G. N. (2010). The physiology of climate change: how potentials for acclimatization and genetic adaptation will determine 'winners' and 'losers'. *J. Exp. Biol.* **213**, 912-920. doi:10.1242/jeb.037473
- Somero, G. N., Lockwood, B. L. and Tomanek, L. (2017). *Biochemical Adaptation: Response to Environmental Challenges, from Life's Origins to the Anthropocene*. Sinauer Associates, Incorporated Publishers.
- Tadros, W. and Lipshitz, H. D. (2009). The maternal-to-zygotic transition: a play in two acts. *Development* **136**, 3033-3042. doi:10.1242/dev.033183
- Tresguerres, M. (2016). Novel and potential physiological roles of vacuolar-type H⁺-ATPase in marine organisms. *J. Exp. Biol.* **219**, 2088-2097. doi:10.1242/jeb.128389
- Trudgill, D., Honek, A., Li, D. and Van Straalen, N. (2005). Thermal time—concepts and utility. *Ann. Appl. Biol.* **146**, 1-14. doi:10.1111/j.1744-7348.2005.04088.x
- Van Vuuren, D. P., Edmonds, J., Kainuma, M., Riahi, K., Thomson, A., Hibbard, K., Hurtt, G. C., Kram, T., Krey, V. and Lamarque, J.-F. (2011). The representative concentration pathways: an overview. *Clim. Change* **109**, 5. doi:10.1007/s10584-011-0148-z
- Varsamos, S., Nebel, C. and Charmantier, G. (2005). Ontogeny of osmoregulation in postembryonic fish: a review. *Comp. Biochem. Physiol. A Mol. Integr. Physiol.* **141**, 401-429. doi:10.1016/j.cbpb.2005.01.013
- Venables, W. N. and Ripley, B. D. (2002). *Modern Applied Statistics with S*, Fourth edition. New York: Springer.
- Waters, J. F. and Millero, F. J. (2013). The free proton concentration scale for seawater pH. *Mar. Chem.* **149**, 8-22. doi:10.1016/j.marchem.2012.11.003
- Wieland, K., Waller, U. and Schnack, D. (1994). Development of Baltic cod eggs at different levels of temperature and oxygen content. *Dana (Charlottenlund)* **10**, 163-177.
- Zalik, S. E., Lewandowski, E., Kam, Z. and Geiger, B. (1999). Cell adhesion and the actin cytoskeleton of the enveloping layer in the zebrafish embryo during epiboly. *J. Biochem. Cell Biol.* **77**, 527-542. doi:10.1139/o99-058